Incongruent reduction of tungsten carbide by a zirconium-copper melt

Zbigniew Grzesik,[a] Matthew B. Dickerson, and Ken H. Sandhage[b]
Department of Materials Science and Engineering, The Ohio State University, Columbus, Ohio 43210

(Received 17 January 2003; accepted 12 June 2003)

The reduction of tungsten carbide (WC) to elemental tungsten by reaction with a Zr–Cu melt was examined. Dense WC disks were immersed in a vertical orientation in molten Zr_2Cu at 1150–1400 °C for 1.5–24 h. Continuous, adherent layers of W and ZrC formed at WC/melt interfaces. The rates of thickening of the W and ZrC product layers were examined as a function of reaction time and temperature and position along the vertical WC surface. Such kinetic data, along with microstructural analyses, indicate that the incongruent reduction of tungsten carbide is likely to be controlled by carbon diffusion through one or both of the product layers.

I. INTRODUCTION

Composite materials comprised of refractory metals (e.g., W, Mo, Ta, Re) and carbides (e.g., HfC, ZrC, TiC, TaC) can possess attractive combinations of chemical, thermal, and mechanical properties.[1–9] Such composites can have higher hardness, greater resistance to wear and creep, and reduced weight relative to refractory metals, and can also exhibit higher fracture strengths, higher toughnesses, and improved thermal shock resistance relative to monolithic carbides. Hence, these materials can be attractive for a variety of applications in the aerospace/aircraft, automotive, energy production, materials processing, defense, and other industries.[7–11]

Among the most extreme environments in aerospace applications can be found in the throat regions of solid-fueled rockets, where combustion products can exceed 2500 °C and flow at supersonic velocities.[9,10] Although refractory metals, such as W and Re (T_m[W] = 3422 °C, T_m[Re] = 3186 °C), may be used under such conditions, these materials possess high specific densities (ρ[W] = 19.3×10^3 kg/m^3, ρ[Re] = 21.0×10^3 kg/m^3).[9,12,13] Refractory metal/carbide composites, such as W/ZrC composites, can be attractive alternatives to pure refractory metals. A composite comprised of equal volumes of W and ZrC is 33% lighter than pure W (12.9×10^3 versus 19.3×10^3 kg/m^3).[13] Such composites are also thermally, chemically, and mechanically compatible. Unlike most metal/ceramic composites, the average linear thermal expansion coefficients of W and ZrC are similar at 20 °C (4.5×10^{-6}/K versus 4.0×10^{-6}/K, respectively) and at 2700 °C (9.2×10^{-6}/K versus 10.2×10^{-6}/K, respectively).[4,5] As a result, W/ZrC composites have exhibited excellent resistance to thermal shock at surface heating rates of ≈2000 °C/s.[8] Like tungsten, zirconium carbide melts at a high temperature (i.e., up to 3445 °C).[3] ZrC and W exhibit limited mutual solid solubilities and do not form intermediate compounds.[3] ZrC can endow a co-continuous W/ZrC composite with enhanced resistance to high-temperature creep and erosion, whereas W can act as a ductile reinforcement at high temperatures for enhanced toughness.[2,6–8]

Dense, co-continuous W/ZrC composites have been produced by the hot pressing of powder mixtures.[7,8] However, the high temperatures (≥2000 °C) and pressures, along with subsequent machining required to generate more complex, nonaxisymmetric shapes, render such processing relatively expensive. An attractive alternative to such conventional processing is the displacive compensation of porosity (DCP) method.[14–17] The DCP method involves the reactive infiltration of a metallic liquid into a rigid, porous, ceramic-bearing preform at ambient pressure. The liquid undergoes an incongruent reduction reaction with a ceramic phase in the preform to yield a ceramic product of larger volume. (Note: Incongruent reduction occurs when a solid ceramic is converted by reduction into solid and liquid products of different composition than the original solid ceramic.[18]) If the starting porous preform is rigid (i.e., consists of a continuous network of necked particles), then the external shape and dimensions of the preform are retained as the internal pore spaces become filled. The DCP process has recently been used to produce W/ZrC-bearing composites.[15] Molten Zr_2Cu was infiltrated into rigid, porous

[a]Present address: Solid State Chemistry Department, Faculty of Materials Science & Ceramics, University of Mining & Metallurgy, al. A. Mickiewicza 30, 30-059 Krakow, Poland.
[b]Address all correspondence to this author.
Present address: School of Materials Science and Engineering, Georgia Institute of Technology, 711 Ferst Drive, Atlanta, GA 30332-0245.
e-mail: ken.sandhage.1@mse.gatech.edu

 © 2003 Materials Research Society

WC preforms, whereupon the Zr_2Cu reacted with WC to yield solid ZrC and W, along with a Cu-rich liquid. Dense, near-net-shaped W/ZrC-bearing composites were generated at only 1200–1300 °C.

Although dense, near-net-shaped refractory metal/carbide composites have been fabricated by the DCP method, the kinetic mechanisms of incongruent reduction are not well understood. The purpose of this paper is to determine the rate-limiting step(s) associated with the incongruent reduction of dense tungsten carbide WC by reaction with molten Zr_2Cu at 1150–1400 °C.

II. EXPERIMENTAL

Incongruent reduction experiments were conducted by immersing dense disks of WC into a molten bath of Zr_2Cu. Dense WC disks were prepared by hot isostatic pressing of WC powder. The WC powder possessed an average particle size (d_{50}) of 0.88 μm and a purity of >99.5% (Alfa Aesar, Johnson Matthey, Ward Hill, MA). The WC powder was mixed with 3 wt.% of an aqueous 10 wt.% solution of polyvinyl alcohol and then uniaxially pressed into disks (13 mm in diameter, ≈3 mm in thickness) at a peak stress of 3×10^8 Pa. The green disks were heated for 4 h at 400 °C in flowing argon, to remove the polyvinyl alcohol, and then for 4 h at 1400 °C. The specimens were further heated for 1 h at 1850 °C under an argon pressure of 7×10^4 Pa, and then hot isostatically pressed at an argon pressure of 2.1×10^8 Pa at 1850 °C for 1 h. The WC disks were polished using a series of SiC abrasive papers and diamond pastes to a surface finish of 0.25 μm. To reveal the grain structure, polished WC cross sections were thermally etched at 1400 °C for 4 h in flowing argon. The argon gas used at the various stages of processing discussed above was passed through a titanium getter (Oxy-gon Industries, Epsom, NH), so that the oxygen partial pressure was reduced to $\leqslant 3 \times 10^{-5}$ Pa.

Zr_2Cu was prepared using Zr sponge (99.6% purity, 0.8–19 mm pieces, Johnson-Matthey) and Cu pieces (99.99% purity, ≈1 mm diameter, Atomergic Chemetals, Farmingdale, NY) as precursors. These materials were placed within a magnesia crucible and heated to 1300 °C for 4–8 h in an oxygen-gettered argon atmosphere. The resulting ingot was crushed into pieces of a few millimeters in diameter and then remelted under similar conditions. X-ray diffraction (XRD) analyses confirmed that the final ingots were comprised of Zr_2Cu.

Prior to an immersion experiment, the hot-isostatically-pressed WC disks were positioned vertically within a magnesia holder inside a magnesia crucible, as shown in the schematic of Fig. 1(a). The disk was surrounded by solid pieces of Zr_2Cu. For each experiment, the molar ratio of Zr_2Cu to WC within the crucible was 18 ± 1. After purging the furnace with flowing, oxygen-gettered argon for 1 h, the furnace was heated to the target temperature (in the range of 1150–1400 °C) and held for a time ranging from 1.5 to 24 h. After cooling, the WC specimens, along with adjacent, adherent solidified melt, were cross sectioned and polished to a surface finish of 0.25 μm. For each reaction temperature and time, the average thicknesses of product layers formed at WC/Zr–Cu interfaces were evaluated by dividing the area of each product layer, obtained by image analyses (3.0.027 software, Clemex Vision, Langueuil, Quebec, Canada) of backscattered electron images, by the length of the interface.

III. RESULTS

After hot isostatic pressing, the tungsten carbide specimens possessed bulk densities of 15.55 (±0.08) × 10^3 kg/m^3, which corresponded to 99.2 ± 0.5% of the theoretical value for WC (15.67 × 10^3 kg/m^3). XRD analysis, and a secondary electron image of a thermally etched cross-section of a hot-isostatically-pressed WC specimen, are shown in Figs. 2(a) and 2(b), respectively. The XRD pattern revealed predominant diffraction peaks for hexagonal WC. Diffraction peaks for α–W_2C or graphite (for C-poor or C-rich compositions, respectively) were not detected, although a trace amount of a cubic WC_{1-x} phase may have been present.[13] Secondary electron images of etched cross sections revealed dense WC specimens with an average grain size of 1.5 μm.

Backscattered electron images of polished cross sections of a specimen exposed to molten Zr_2Cu for 1.5 h at 1400 °C are shown in Fig. 1(b). For each cross section, a relatively bright reaction product layer was observed adjacent to the unreacted WC. This bright layer was separated from the solidified Zr_2Cu by a relatively dark product layer. Energy dispersive x-ray analyses indicated that the relatively bright layer was comprised of tungsten, whereas the dark layer was comprised of zirconium carbide. Examination of similar cross sections obtained from other specimens revealed that the W and ZrC product layers forming on WC increased in thickness as a function of exposure time to the Zr_2Cu melt. The squares of the average W and ZrC layer thicknesses are plotted against reaction time in Figs. 3(a) and 3(b). For each reaction temperature, the data points exhibited a good fit to parabolic kinetics. The cross sections shown in Fig. 1(b) were obtained from locations near the top and bottom of the vertically oriented specimen, respectively [Fig. 1(a)]. The average thicknesses of the W and ZrC layers formed at the top and bottom locations were similar. The thicknesses of product layers formed at other temperatures and times were also observed to be independent of vertical position along the specimen surfaces.

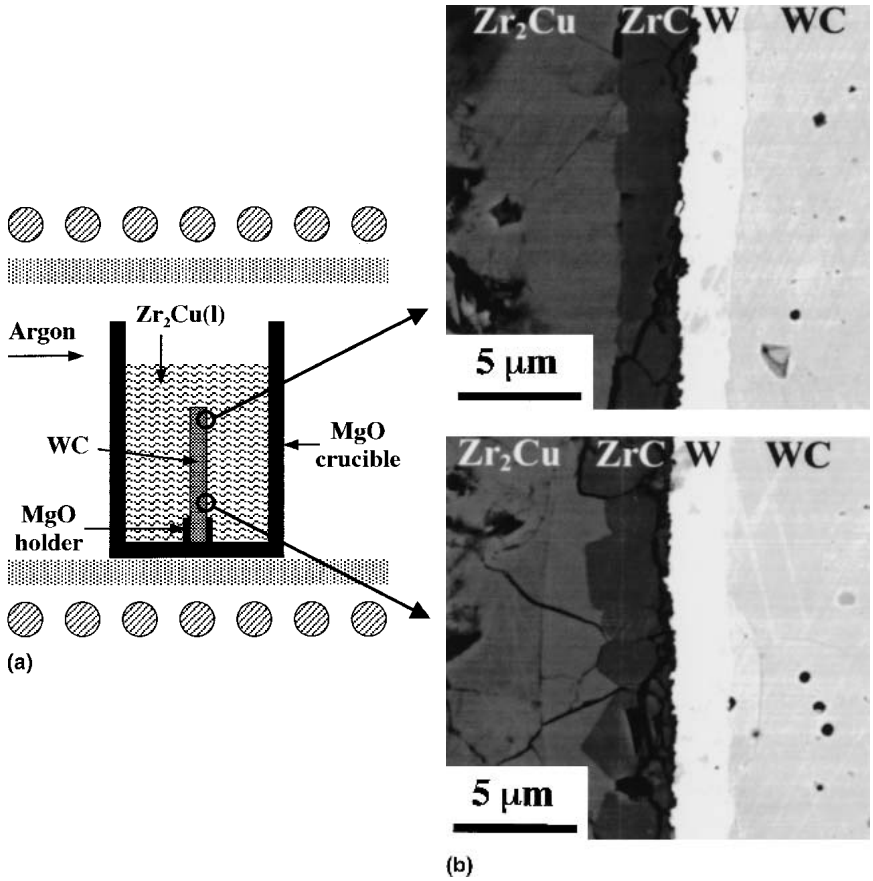

FIG. 1. (a) Experimental setup for the immersion of dense WC disks in molten Zr_2Cu. (b) Backscattered electron images of polished cross sections of dense WC after reaction with molten Zr_2Cu for 1.5 h at 1400 °C. These images were obtained at various locations along the surface of the vertically immersed WC specimens, as shown in the schematic.

The slopes of the lines shown in Figs. 3(a) and 3(b) were used to obtain the parabolic rate constants (K_p values) for the thickening of the tungsten and zirconium carbide layers at each reaction temperature.[19] The logarithms of the parabolic rate constants are plotted against the inverse of temperature in Fig. 4. For each product layer, the data points exhibited a good fit to Arrhenius behavior. The activation energies, obtained from the slopes of these lines, were virtually the same for the growth of the tungsten (263 kJ/mol) and zirconium carbide (247 kJ/mol) layers.

For immersion times up to 24 h at temperatures of 1150–1400 °C, continuous layers of W and ZrC tended to form on the WC specimens. However, infrequent, isolated discontinuities in the zirconium carbide layer resulted in the exposure of the tungsten layer to the zirconium-bearing melt, as shown in Fig. 5. Enhanced consumption of the WC specimen was observed (i.e., pits formed in the WC) at these locations [Fig. 5(c)]. Within these pits, the thickness of the tungsten layer was locally reduced, and discontinuous particles of W_2Zr formed [Figs. 5(b) and 5(c)].

IV. DISCUSSION

Exposure of dense WC specimens to molten Zr_2Cu at 1150–1400 °C resulted in the following net incongruent reduction reaction:

$$1/2Zr_2Cu(l) + WC(s) \rightarrow W(s) + ZrC(s) + 1/2(Cu) \quad , \quad (1)$$

where (Cu) refers to copper dissolved within the excess liquid solution surrounding the specimen. This reaction is strongly favored from a thermodynamic perspective. For example, a thermodynamic calculation using available data for the excess Gibbs free energy of mixing of Zr–Cu melts, and the free energies of formation of ZrC and WC, indicated that this reaction should occur spontaneously at 1300 °C for Zr-Cu melts with >0.092 at.% Zr (i.e., only 920 ppm Zr was required in the melt).[20–22] For the immersion of WC into molten Zr_2Cu at 1300 °C, the Gibbs free-energy change for Reaction (1) was calculated to be −135.2 kJ/mol.[20–22]

A corrosion process is generally considered to be "passive" if a continuous, adherent, solid product layer forms on the corroding solid surface, so as to physically separate the corroding solid from the reactive fluid and

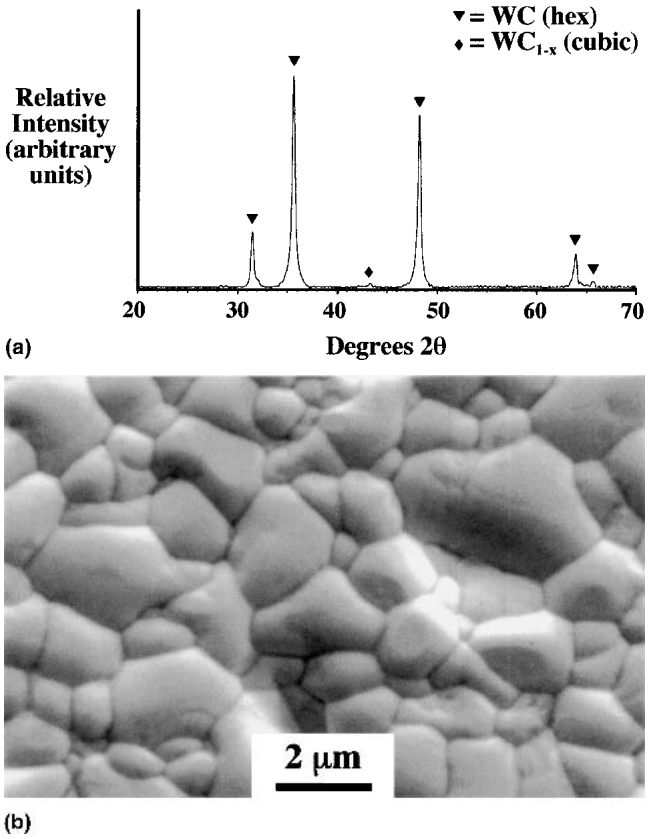

FIG. 2. (a) XRD analysis of a hot isostatically pressed WC specimen. (b) Secondary electron image of a thermally etched cross section of a hot isostatically pressed WC specimen.

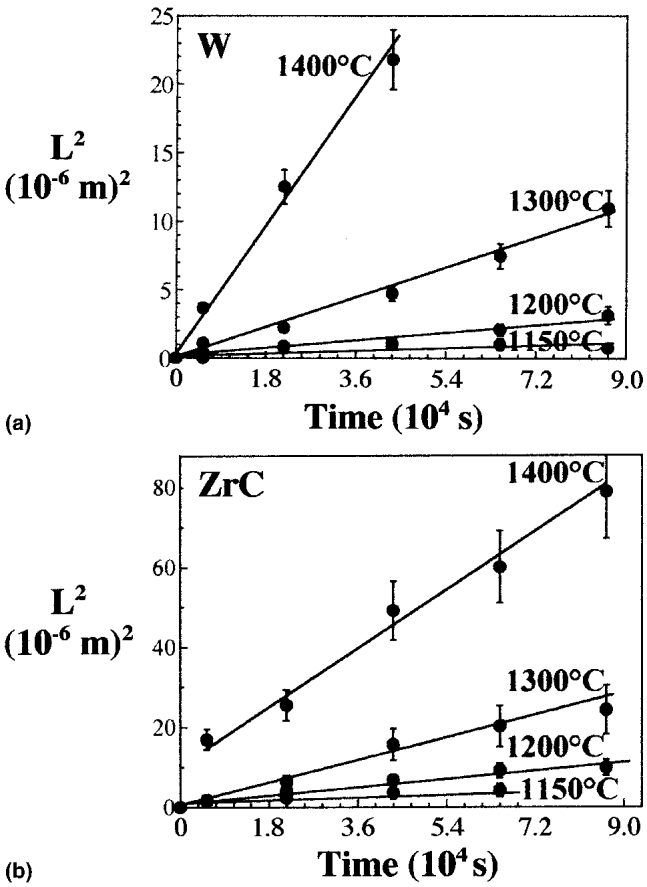

FIG. 3. Plots of the square of the layer thickness L^2 versus reaction time for the (a) W and (b) ZrC product layers formed on WC upon immersion in Zr_2Cu(l) at 1150–1400 °C.

thereby slow the rate of corrosion.[23] In the present work, the W and ZrC products of Reaction (1) generally formed as continuous, adherent layers on the underlying dense WC. By analogy to other types of corrosion, such ZrC and W layer formation on WC may be considered to be an example of "passive incongruent reduction." At locations where the ZrC layer was not continuous, the underlying W layer reacted with the melt to form discontinuous particles of W_2Zr (Fig. 5). At these locations, the rate of consumption of the WC was locally enhanced, so that pits formed on the specimen surface [Fig. 5(c)]. Such accelerated reaction due to the formation of discontinuous (and apparently less protective) ZrC and W_2Zr products is an example of "active incongruent reduction."

During passive incongruent reduction in molten Zr_2Cu, the WC was physically separated from the melt by layers of W and ZrC. In the present experiments, excess amounts of the reactants, Zr_2Cu(l) and WC(s), were used to avoid depletion of these reactants during the course of a given experiment. For example, under the most extreme reaction condition of 1400 °C for 24 h, less than 0.03 at.% of the zirconium available in the melt, and less than 0.9 at.% of the carbon available in the WC specimen, were consumed to produce the ZrC and W layers. Under these conditions, the rate of passive incongruent reduction of WC could have been limited by one or more of the following steps: (i) solid-state diffusion (through the WC specimen, or through the W or ZrC product layers), (ii) liquid phase diffusion, (iii) a chemical reaction (at the WC/W, W/ZrC, or ZrC/melt interfaces).

The formation of W and ZrC layers on planar WC specimens during immersion in molten Zr_2Cu resulted in very little change in the surface area of the planar WC specimens ($\leqslant$0.3%). As seen in Figs. 3(a) and 3(b), the tungsten and zirconium carbide layers increased in thickness at parabolic rates for all of the temperatures examined. Such parabolic kinetics are not consistent with chemical reaction control; that is, with essentially constant interfacial areas and reactant concentrations, chemical reaction control should have resulted in linear kinetics.[19]

The parabolic rate constants for the thickening of the tungsten and zirconium carbide layers followed Arrhenius behavior (Fig. 4). The similar values of activation energy obtained for W and ZrC layer growth (263 and

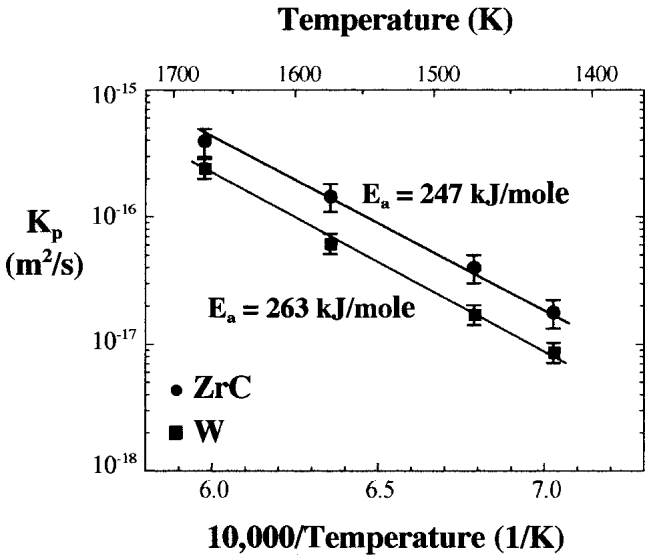

FIG. 4. Plot of the parabolic rate constants K_p for thickening of the W and ZrC product layers as a function of inverse temperature (E_a = activation energy).

247 kJ/mol, respectively) suggested that the steady-state growth of both layers was controlled by a common mechanism. These activation energies were considerably higher than values reported for the diffusion of copper or zirconium in molten copper or in Zr–Cu-bearing liquids.[24,25] Furthermore, a change in the melt density near the WC/melt interface, due to the selective removal of zirconium from the melt by Reaction (1), should have resulted in convection in the melt. If liquid-phase diffusion was the rate-limiting step, then such density-driven free convection in the vicinity of a vertical plate should have led to a steady-state reaction rate that was independent of time, but dependent on vertical position.[26] However, the present results indicated that the product layer thickening rates were independent of position [Fig. 1(b)] and dependent on time (Fig. 3). Hence, mass transport through the liquid is unlikely to be the rate-limiting step.

Activation energies reported for diffusion through WC, W, and ZrC are shown in Table I.[27–32] The activation energies reported for the lattice diffusion of zirconium and carbon through ZrC (719 and 473 kJ/mol, respectively[27,28]) were significantly higher than the values obtained in the present work. However, the activation energies associated with the diffusion of carbon (Table I) along grain boundaries in WC and ZrC, or through the lattice of tungsten, agreed reasonably well with the values shown in Fig. 4.[28–31] At locations where the ZrC layer was not continuous, the WC was observed to undergo an enhanced rate of reaction [i.e., a pit formed in the WC specimen, as shown in Fig. 5(c)]. At such regions of active incongruent reduction, the thickness of the tungsten layer was locally reduced and discrete particles of W_2Zr formed. Such enhanced local reaction (pitting)

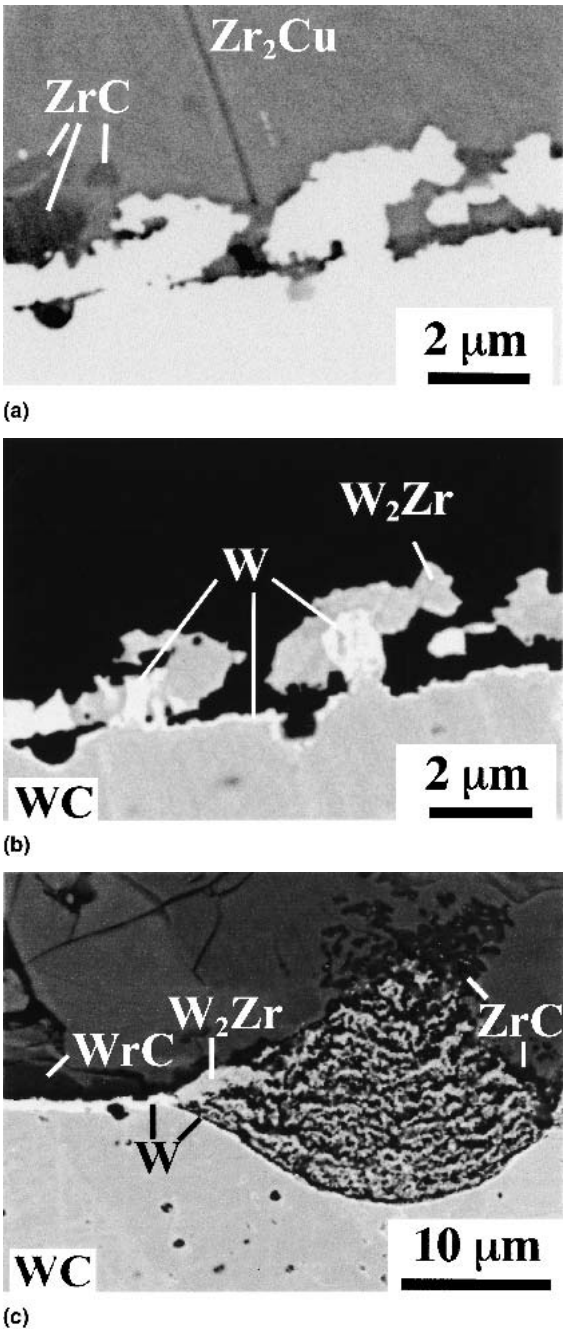

FIG. 5. (a,b) High-magnification backscattered electron images revealing the formation of W_2Zr particles at locations where the ZrC product layer was not continuous. (Note: two images of the same location are shown with different contrasts to reveal the ZrC, W, and W_2Zr phases.) (c) A lower magnification backscattered electron image, relative to (a) and (b), revealing the formation of a pit in the WC surface. Appreciable W_2Zr particle formation is observed in the vicinity of the pit.

should not have occurred if carbon diffusion through the tungsten carbide was rate limiting. Hence, these results indicate that the rate-limiting step for the passive incongruent reduction of tungsten carbide is likely to be the

TABLE I. Activation energies (kJ/mol) reported for grain boundary (GB) or lattice diffusion of carbon (C^{14}) and zirconium (Zr^{95}) through WC, W, and ZrC.[27–32]

C^{14}						Zr^{95}
WC		W		ZrC		ZrC
GB	Lattice	GB	Lattice	GB	Lattice	Lattice
297	368	169	207	288–376	473	719

solid-state diffusion of carbon through the lattice of the tungsten product layer and/or through grain boundaries in the zirconium carbide product layer.

V. CONCLUSIONS

The exposure of dense, vertically oriented disks of WC to molten Zr_2Cu at 1150–1400 °C for 1.5–24 h resulted in the formation of continuous, adherent layers of W and ZrC on the WC surface. The effects of time, temperature, and vertical position on the thickening rates of the W and ZrC product layers, and the influence of infrequent disruptions in these product layers on the local WC consumption rate, indicate that the passive incongruent reduction of WC is likely to be controlled by solid-state diffusion of carbon through the lattice of the W layer and/or through grain boundaries in the ZrC layer.

ACKNOWLEDGMENTS

This work was supported by the Air Force Office of Scientific Research (Grant Nos. F49620-01-1-0477 and F49620-02-1-0349; Dr. Joan Fuller, Program Manager). Support for one of the authors (Z. Grzesik) was also provided by the J. William Fulbright Foundation.

REFERENCES

1. E.K. Storms, *The Refractory Carbides* (Academic Press, New York, 1967), pp. 18–35.
2. W.S. Williams, in *Progress in Solid State Chemistry,* edited by H. Reiss and J.O. McCaldin (Pergamon Press, New York, 1971), Vol. 6, pp. 57-118.
3. *Phase Equilibria Diagrams, Vol. X. Borides, Carbides, and Nitrides,* edited by A.E. McHale (The American Ceramic Society, Westerville, OH, 1994), pp. 251–252, 257–260, 265–271, 274, 291, 292, 294–300, 303, 304, 313–315, 317–322, 349–360, 365–368, 371.
4. Y.S. Touloukian, R.K. Kirby, R.E. Taylor, and P.D. Desai, *Thermal Expansion Metallic Elements and Alloys* (Plenum Press, New York, 1975), Vol. 12, pp. 208–218, 236–240, 280–284, 316–322, 354–364.
5. Y.S. Touloukian, R.K. Kirby, R.E. Taylor, and T.Y.R. Lee, *Thermal Expansion Nonmetallic Solids* (Plenum Press, New York, 1977), Vol. 13, pp. 848–852, 858–865, 879–883, 891–895, 926–934.
6. *Properties and Selection: Stainless Steels, Tool Materials and Special-Purpose Materials,* Metals Handbook, 9th ed., Vol. 3, (American Society for Metals, Metals Park, OH, 1980), pp. 314–349.
7. G.M. Song, Y.J. Wang, and Y. Zhou, Mater. Sci. Eng. A **A334,** 223 (2002).
8. G.M. Song, Y.J. Wang, and Y. Zhou, J. Mater. Sci. **36,** 4625 (2001).
9. K. Upadhya, J-M. Yang, and W.P. Hoffman, Bull. Am. Ceram. Soc. **76,** 51 (1997).
10. G.P. Sutton, *Rocket Propulsion Elements: An Introduction to the Engineering of Rockets*, 6th ed. (John Wiley & Sons, New York, 1992), pp. 483–488.
11. L.M. Sheppard, Bull. Am. Ceram. Soc. **69,** 1012 (1990).
12. Z.K. Liu and Y.A. Chang, J. Alloys Compd. **299,** 153 (2000).
13. Powder Diffraction Files Card Nos. 4-806 for W, No. 5-702 for Re, 25-1047 for WC(hexagonal), 20-1316 for WC_{1-x}(cubic), 35-784 for ZrC, 4-826 for Cu, and 18-466 for Zr_2Cu (International Center for Diffraction Data, Newtown Square, PA, 1981).
14. K.H. Sandhage and P. Kumar, U.S. Patent No. 6 407 022 (June 18, 2002).
15. M.B. Dickerson, R.L. Snyder, and K.H. Sandhage, J. Am. Ceram. Soc. **85,** 730 (2002).
16. P. Kumar and K.H. Sandhage, J. Mater. Sci. **34,** 5757 (1999).
17. K.A. Rogers, P. Kumar, R. Citak, and K.H. Sandhage, J. Am. Ceram. Soc. **82,** 757 (1999).
18. P. Kumar, S.A. Dregia, and K.H. Sandhage, J. Mater. Res. **14,** 3312 (1999).
19. P. Kofstad, *High Temperature Corrosion* (Elsevier Applied Science, New York, 1988), pp. 11–25.
20. N. Saunders, CALPHAD **9,** 297 (1985).
21. O.J. Kleppa and S. Watanabe, Metall. Trans. B. **13B,** 391 (1982).
22. I. Barin, *Thermochemical Data of Pure Substances,* 3rd ed. (VCH Verlagsgesellschaft, Weinheim, Germany, 1995), pp. 1788, 1860.
23. D.A. Jones, *Principles and Prevention of Corrosion,* 2nd ed. (Prentice Hall, Upper Saddle River, NJ, 1996), p. 116.
24. C. Gaukel, M. Kluge, and H.R. Schober, J. Non-Cryst. Solids. **250–252,** 664 (1999).
25. J. Henderson and L. Young, Trans. Metall. Soc. AIME. **221,** 72 (1961).
26. C. Wagner, J. Phys. Colloid Chem. **53,** 1030 (1949).
27. R.A. Andrievskii, Yu. F. Khromov, and I.S. Alekseeva, Fiz. Metal. Metalloved. **32,** 664 (1971).
28. S. Sarian and J.M. Criscione, J. Appl. Phys. **38,** 1794 (1967).
29. C.P. Buhsmer and P.H. Crayton, J. Mater. Sci. **6,** 981 (1971).
30. Yu. N. Vilk, S.S. Nikolskii, and R.G. Avarbe, Teplofiz. Vys. Temp. **5,** 607 (1967).
31. A. Shepela, J. Less-Common Met. **26,** 33 (1972).
32. I. Kovenskii, in *Diffusion in Body-Centered Cubic Metals* (American Society for Metals, Metals Park, OH, 1965), p. 283.